International Conference on Control, Automation and Systems 2008
Oct. 14-17, 2008 in COEX, Seoul, Korea

On Position Control using GMS-Model-Based Friction Compensation and Velocity Reduced-Order Observer for Servo-Systems - LMI Approach

Karim Khayati[1]

[1]Department of Mechanical Engineering, Royal Military College (RMC), Kingston (ON), CANADA
(Tel : +1-613-541-6000 #8407; E-mail: karim.khayati@rmc.ca)

Abstract: This paper is devoted to a stabilization problem for a servo-system under the influence of friction. The proposed approach is based on a multi-objective control design using a reduced-order velocity observer, a generalized Maxwell-slip (GMS) model-based friction compensation and a linear time invariant (LTI) compensator simultaneously. Stabilization conditions on interconnected systems are investigated with strictly positive real (SPR) condition on linear closed-loop dynamics of hierarchical systems using linear matrix inequality (LMI) frameworks. The appeal of this proven theoretical design is further demonstrated by numerical results.

Keywords: Position control, Reduced-order velocity observer, Friction compensation, GMS model, Stabilization, SPR condition, Hierarchical systems, Interconnected systems, Multi-objective design, LMI.

1. INTRODUCTION

The unavoidable friction phenomena cause in general the performance of servomechanisms to deteriorate due to non negligible tracking errors, limit cycles and undesired stick-slip motion [1]. They pay out nearly all machines incorporating moving parts (robots, electromechanical systems, pneumatic actuators, etc.). So, several strategies have been investigated in the literature (see e.g. [2], [3] and references cited therein) to address this issue, with a view to achieving a higher degree of servo-system accuracy without the need for excessive integral gains. In this paper, we apply the nonlinear GMS-based friction compensation and the linear position tracking schemes presented in [5] within a velocity estimation design. Since only position measurements are available, the velocity has to be estimated using a reduced-order observer [4]. The dynamic GMS friction model captures most friction characteristics and generically maps the macroscopic behavior of the friction force as better as the microscopic contact force between asperities and irregularities characterizing the surfaces during motion [6]. The stabilization conditions are cast as a convex problem of multi-objective output feedback controller involving LMIs [7]. Simulation results illustrate the effectiveness of the proposed control design.

This paper is organized as follows. Section 2 introduces the model of a moving single mass with friction. We briefly recall the above-mentioned GMS model. In section 3, we investigate the observer-based control design. A multi-objective output feedback synthesis is then presented in section 4. Simulations are presented in section 5. Finally, concluding remarks appear in section 6.

2. PROBLEM STATEMENT

Here, we investigate a single mass m at a position x moving with a velocity $v = \dot{x}$ under the influence of an input force F and a dynamic friction force F_f:

$$m\ddot{x} = F - F_f \tag{1}$$

The dynamic friction model we consider is the multi-state GMS friction one [6]:

$$\begin{aligned} \dot{z}_i &= \begin{cases} v & \text{until } z_i = s_i(v) \\ \mathrm{sgn}(v)C_i(1 - \frac{z_i}{s_i(v)}) & \text{until } v = 0 \end{cases} \\ F_f &= \sum_{i=1}^{N} \gamma_i z_i + \sum_{i=1}^{N} \delta_i \dot{z}_i + bv + \omega_d \\ s_i(v) &= \frac{\mathrm{sgn}(v)}{\gamma_i}(f_{c_i} + (f_{s_i} - f_{c_i}) \cdot e^{-\theta_s |v|^{\delta_s}}) \end{aligned} \tag{2}$$

where C_i is the attraction parameter, *i.e.* the gain that determines how fast z_i converges to the Stribeck friction s_i, γ_i the stiffness coefficient, δ_i the viscoelastic coefficient, b the viscous friction coefficient, f_c the Coulomb friction force, f_s the static friction, θ_s the reciprocal Stribeck velocity, δ_s an arbitrary exponent and ω_d a priori bounded disturbance due to unmodelled friction variations (*i.e.* extra or lacking number of GMS stages).

The controller design presented in the next section is based on the following assumptions: **(A.1)** The position x is assumed to be measurable. **(A.2)** The velocity v, the internal states z_i and the resultant friction force are physically non measurable. **(A.3)** The dynamic model (1) and (2) is well characterized by the known parameters b, f_{c_i}, f_{s_i}, m, γ_i, δ_i, δ_s and θ_s.

The control objective is to design a compensator to track any prescribed smooth trajectory by using the velocity estimate provided by a reduced-order observer instead of the actual velocity, and to eliminate the friction force effect by using a GMS-model-based feedback observer.

3. CONTROL STRATEGY

In this section, we introduce (see Fig. 1):

- a reduced-order observer to estimate the velocity,
- a model-based friction compensator to reduce the effect of friction, and
- an LTI compensator to ensure an accurate positioning performance.

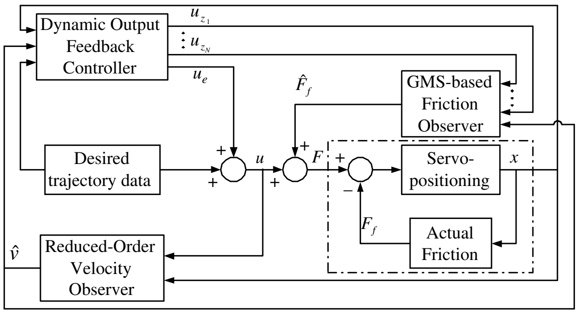

Fig. 1 Block diagram of the Model-based friction compensation scheme with velocity estimation.

3.1 Reduced-order velocity observer

The reduced-order observer dynamics we propose is

$$\dot{\hat{v}} = \frac{\kappa}{m} \cdot (v - \hat{v}) + \frac{1}{m}u = \frac{\kappa}{m} \cdot \tilde{v} + \frac{1}{m}u \tag{3}$$

with κ is the observer gain. But, since Eq. (3) depends on the unmeasured velocity v, it is not directly applicable in practice. For implementation purposes, we propose the modified observer state $\breve{v} = \hat{v} - \frac{\kappa}{m}x$ for which the dynamics depends only on the measured position as follows

$$\dot{\breve{v}} = -\frac{\kappa}{m}\breve{v} + \frac{1}{m}u - (\frac{\kappa}{m})^2 x \tag{4}$$

We note that from now on, for the simplicity of the stability proof, we will consider the Eq. (3) exclusively.

3.2 GMS-model-based friction observer

Under assumptions (A.2) and (A.3), let the observer-based friction compensation scheme be given by:

$$\dot{\hat{z}}_i = \begin{cases} \hat{v} - u_{z_i} & \text{until } \hat{z}_i = s_i(v) \\ \mathrm{sgn}(\hat{v})C_i(1 - \frac{\hat{z}_i}{s_i(\hat{v})}) - u_{z_i} & \text{until } \hat{v} = 0 \end{cases} \tag{5}$$

and

$$\hat{F}_f = \sum_{i=1}^{N} \gamma_i \hat{z}_i + \sum_{i=1}^{N} \delta_i \dot{\hat{z}}_i + b\hat{v} \tag{6}$$

where $\hat{z}_i$ is the ith observed internal state and u_{z_i} constitutes any observer feedback term in the ith-GMS-stage model related to the positioning and the velocity estimation error dynamics.

3.3 Feedback friction-observer-based controller design

In this section, we introduce the actual input of the dynamics (1). It is given by (see Fig. 1):

$$F = u + \hat{F}_f = m\ddot{x}_d + u_e + \hat{F}_f \tag{7}$$

where u_e designates a direct active force and is any dynamic controller term related to the measurable/observable states of the system.

3.4 Closed-loop error dynamics

We introduce the trajectory tracking and observation errors respectively:

$$\begin{aligned} &e_x = x_d - x \;; \quad e_v = v_f - \hat{v} \;; \quad v_f = v_d + k_s e_x \;; \\ &\tilde{z}_i = z_i - \hat{z}_i \;; \quad \tilde{F}_f = F_f - \hat{F}_f \end{aligned} \tag{8}$$

From the filtered velocity tracking error e_v, we have:

$$\tilde{v} = v - \hat{v} = e_v - \dot{e}_x - k_s e_x \tag{9}$$

To compute the error dynamics for the friction observer, four different scenarios (or cases) can be distinguished. Both the elementary real model and the observer are sticking (case 1), or both the elementary real model and the observer are slipping (case 2). And possibly, the real friction and the observer one behave differently on behalf few moments. So, one situation is given when the elementary real model is sticking and the observer is slipping (case 3), and another situation may take place when the elementary real model is slipping and the observer is sticking (case 4). Then, we have

$$\dot{\tilde{z}}_i = \begin{cases} \omega_{z_i} + u_{z_i} & \text{cases 1 \& 4} \\ -C_i \frac{\mathrm{sgn}(\hat{v})}{s_i(\hat{v})}\tilde{z}_i + \omega_{z_i} + u_{z_i} & \text{cases 2 \& 3} \end{cases} \tag{10}$$

with ω_{z_i} is equal to $v - \hat{v}$ in case 1, $(\mathrm{sgn}(v)(1 - \frac{z_i}{s_i(v)}) - \mathrm{sgn}(\hat{v})(1 - \frac{\mathrm{sgn}(\hat{v})}{s_i(\hat{v})} z_i))C_i$ in case 2, $v - \mathrm{sgn}(\hat{v})C_i(1 - \frac{z_i}{s_i(\hat{v})})$ in case 3 and $\mathrm{sgn}(v)C_i(1 - \frac{z_i}{s_i(v)}) - \hat{v}$ in case 4. The phases 3 and 4 remain occasional and are characterized by well-finite actual and/or estimated velocity magnitudes, as either the friction process or the estimator one is sticking during these eventual phases. Since the internal friction states z_i of the GMS modelization are bounded [6] and based on the bound velocity behavior during any sticking phase, ω_{z_i} is then supposed to be a bounded exogenous input signal.

From now on, we denote by $\tilde{\mathbf{z}} = \begin{pmatrix} \tilde{z}_1 & \dots & \tilde{z}_N \end{pmatrix}^{\mathrm{T}}$ the internal friction error vector. The vector $\mathbf{u}_z = \begin{pmatrix} u_{z_1} & \dots & u_{z_N} \end{pmatrix}^{\mathrm{T}}$ is the friction observer feedback input and is used to enforce the robustness of the friction compensation to the tracking and the observer dynamics. This command-vector will be issued from an LTI compensator that will be established later. Finally, $\omega_{\mathbf{z}} = \begin{pmatrix} \omega_{z_1} & \dots & \omega_{z_N} \end{pmatrix}^{\mathrm{T}}$ designates the exogenous input vector of the friction error dynamics. By convenience for the closed-loop stabilization scheme that will be formulated in the next section, we rewrite the friction error dynamics (10) as follows (Σ_{NL}):

$$\dot{\tilde{\mathbf{z}}} = -\varphi(\hat{v})\tilde{\mathbf{z}} + \mathbf{u}_z + \omega_z \tag{11}$$

where $\varphi(\hat{v}) = \mathbf{diag}(\varphi_1(\hat{v}), \dots, \varphi_N(\hat{v}))$, with

$$\varphi_i(\hat{v}) = \begin{cases} 0 & \text{in cases 1 \& 4} \\ -C_i \frac{\mathrm{sgn}(\hat{v})}{s_i(\hat{v})} & \text{in cases 2 \& 3} \end{cases} \tag{12}$$

Noting that, for all $i = 1, .., N$, $\varphi_i(\hat{v}) \geq 0$. The formulation of the nonlinear error dynamics (11) and (12) is chosen to ensure that the matrical mapping between

$\mathbf{u}_z + \omega_z$ and $\tilde{\mathbf{z}}$ is passive with respect to the storage function $V(t) = \frac{1}{2}\tilde{\mathbf{z}}^{\mathrm{T}}\tilde{\mathbf{z}}$, that is the time derivative of V satisfies

$$\dot{V}(t) = \tilde{\mathbf{z}}^{\mathrm{T}}\dot{\tilde{\mathbf{z}}} \leq \tilde{\mathbf{z}}^{\mathrm{T}}(\mathbf{u}_z + \omega_z) \tag{13}$$

This property will be fundamental for the stability of the system presented later.

From Eqs. (2) and (6), we obtain the resultant friction force error:

$$\begin{aligned} \tilde{F}_f &= \sum_{i=1}^{N} \gamma_i \tilde{z}_i + \sum_{i=1}^{N} \delta_i \dot{\tilde{z}}_i + b\tilde{v} + \omega_d \\ &= \mathbf{\Gamma}^{\mathrm{T}}\tilde{\mathbf{z}} + \mathbf{\Delta}^{\mathrm{T}}\dot{\tilde{\mathbf{z}}} + b\tilde{v} + \omega_d \end{aligned} \tag{14}$$

with $\mathbf{\Gamma} = \begin{pmatrix} \gamma_1 & \ldots & \gamma_N \end{pmatrix}^{\mathrm{T}}$, $\mathbf{\Delta} = \begin{pmatrix} \delta_1 & \ldots & \delta_N \end{pmatrix}^{\mathrm{T}}$.

Using Eqs. (1), (3), (7) and (8), the reduced-order observer error dynamics is given by:

$$m\dot{\tilde{v}} = -\tilde{F}_f - \kappa\tilde{v} \tag{15}$$

The choice of our control results in the following tracking error dynamics:

$$m\ddot{e}_x = -u_e + \tilde{F}_f \tag{16}$$

The compensation terms u_{z_i}; for $i = 1, .., N$; and u_e will be further defined in the following subsection.

3.5 LTI compensator design

Consider the overall closed-loop error dynamics (11), (12), (14) $\sim$ (16). Using (8) and (9), let $\mathbf{x} = \begin{pmatrix} e_x & \dot{e}_x \end{pmatrix}^{\mathrm{T}}$ be the state vector and $\mathbf{u} = \begin{pmatrix} u_e & \mathbf{u}_z^{\mathrm{T}} \end{pmatrix}^{\mathrm{T}}$ the input vector, where u_e is introduced in Eq. (7) and the components of $\mathbf{u}_z$ are introduced in Eq. (5). Under assumptions (A.1) and (A.2), as $\mathbf{x} = \begin{pmatrix} e_x & \dot{e}_x \end{pmatrix}^{\mathrm{T}}$ contains the unknown actual velocity and assuming the well-posed term e_v given in Eq. (8), we propose as known output vector $\mathbf{y} = \begin{pmatrix} e_x & e_v \end{pmatrix}^{\mathrm{T}}$. Therefore, using Eqs. (9), (14) and (16), we rewrite the positioning error dynamics in the state space representation as:

$$\dot{\mathbf{x}} = \mathbf{A}\mathbf{x} + \mathbf{B}\mathbf{u} + \mathbf{B}_\gamma(-\tilde{\mathbf{z}}) + \mathbf{B}_\delta(-\dot{\tilde{\mathbf{z}}}) + \mathbf{B}_v\tilde{v} + \mathbf{B}_d\omega_d \tag{17}$$

and

$$\mathbf{y} = \mathbf{C}\mathbf{x} + \mathbf{D}_v\tilde{v} \tag{18}$$

where $\mathbf{A} = \begin{pmatrix} 0 & 1 \\ 0 & 0 \end{pmatrix}$, $\mathbf{B} = \begin{pmatrix} 0 & \mathbf{0}_{1,N} \\ -\frac{1}{m} & \mathbf{0}_{1,N} \end{pmatrix}$, $\mathbf{B}_v = \begin{pmatrix} 0 \\ \frac{b}{m} \end{pmatrix}$, $\mathbf{B}_\gamma = \begin{pmatrix} \mathbf{0}_{1,N} \\ -\frac{1}{m}\mathbf{\Gamma}^{\mathrm{T}} \end{pmatrix}$, $\mathbf{B}_\delta = \begin{pmatrix} \mathbf{0}_{1,N} \\ -\frac{1}{m}\mathbf{\Delta}^{\mathrm{T}} \end{pmatrix}$, $\mathbf{B}_d = \begin{pmatrix} 0 \\ \frac{1}{m} \end{pmatrix}$, $\mathbf{C} = \begin{pmatrix} 1 & 0 \\ k_s & 1 \end{pmatrix}$ and $\mathbf{D}_v = \begin{pmatrix} 0 \\ 1 \end{pmatrix}$, with $\mathbf{0}_{1,N}$ designates the N-row null vector.

The control vector $\mathbf{u} = \begin{pmatrix} u_e & \mathbf{u}_z^{\mathrm{T}} \end{pmatrix}^{\mathrm{T}}$ is considered the output of any LTI compensator (K), which can be represented in any general state-space form as follows (see Fig. 1):

$$\begin{cases} \dot{\mathbf{x}}_{\mathbf{c}} &= \mathbf{A}_{\mathbf{c}}\mathbf{x}_{\mathbf{c}} + \mathbf{B}_{\mathbf{c}}\mathbf{y} \\ \mathbf{u} &= \mathbf{C}_{\mathbf{c}}\mathbf{x}_{\mathbf{c}} + \mathbf{D}_{\mathbf{c}}\mathbf{y} \end{cases} \tag{19}$$

where $\mathbf{x}_{\mathbf{c}}$ represents a two-dimensional controller state vector. The dynamic controller gains $\mathbf{A}_{\mathbf{c}}$ and $\mathbf{B}_{\mathbf{c}}$ are 2×2-matrices, $\mathbf{C}_{\mathbf{c}}$ and $\mathbf{D}_{\mathbf{c}}$ are is a $(N+1) \times 2$-matrix.

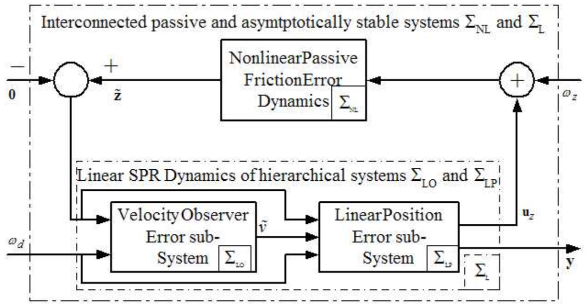

Fig. 2 Interconnected and hierarchical SPR and passive systems.

In the following statement, we establish the overall closed-loop linear dynamics (Σ_{L}) by combining the reduced-order observer dynamics (Σ_{LO}) and the position tracking dynamics (Σ_{LP}), and which will be linked to the nonlinear friction compensation error dynamics (Σ_{NL}).

Proposition 1: Consider the closed-loop linear dynamics stated by Eqs. (14), (15), (17) $\sim$ (19). Then, the overall linear dynamics (Σ_{L}) represented in Fig. 2 is stated as follows:

$$\begin{pmatrix} \dot{\tilde{\mathbf{x}}} \\ \dot{\bar{v}} \end{pmatrix} = \begin{pmatrix} \tilde{\mathbf{A}} & \tilde{\mathbf{B}}_v \\ \mathbf{0}_{1,4} & \tilde{A}_o \end{pmatrix} \begin{pmatrix} \tilde{\mathbf{x}} \\ \bar{v} \end{pmatrix} + \begin{pmatrix} \tilde{\mathbf{B}}_z \\ \tilde{\mathbf{B}}_{oz} \end{pmatrix} (-\tilde{\mathbf{z}}) + \begin{pmatrix} \tilde{\mathbf{B}}_d \\ \tilde{B}_{od} \end{pmatrix} \omega_d \tag{20}$$

$$\mathbf{u}_z = \begin{pmatrix} \tilde{\mathbf{C}}_u & \tilde{\mathbf{C}}_{uv} \end{pmatrix} \begin{pmatrix} \tilde{\mathbf{x}} \\ \bar{v} \end{pmatrix} \tag{21}$$

and

$$\mathbf{y} = \begin{pmatrix} \tilde{\mathbf{C}}_y & \tilde{\mathbf{C}}_{yv} \end{pmatrix} \begin{pmatrix} \tilde{\mathbf{x}} \\ \bar{v} \end{pmatrix} \tag{22}$$

where $\tilde{\mathbf{A}} = \begin{pmatrix} \mathbf{A} + \mathbf{B}\mathbf{D}_{\mathbf{c}}\mathbf{C} & \mathbf{B}\mathbf{C}_{\mathbf{c}} \\ \mathbf{B}_{\mathbf{c}}\mathbf{C} & \mathbf{A}_{\mathbf{c}} \end{pmatrix}$, $\tilde{A}_o = -\frac{b+\kappa}{m}$, $\tilde{\mathbf{B}}_d = \begin{pmatrix} \mathbf{B}_d \\ \mathbf{0}_{2,1} \end{pmatrix}$, $\tilde{\mathbf{B}}_v = \begin{pmatrix} \mathbf{B}_v + \mathbf{B}\mathbf{D}_{\mathbf{c}}\mathbf{D}_v \\ \mathbf{B}_{\mathbf{c}}\mathbf{D}_v \end{pmatrix}$, $\tilde{\mathbf{B}}_z = \begin{pmatrix} \mathbf{B}_z \\ \mathbf{0}_{2,N} \end{pmatrix}$, $\tilde{B}_{od} = -\frac{1}{m}$, $\tilde{\mathbf{B}}_{oz} = \frac{1}{m}\mathbf{\Gamma}^{\mathrm{T}} - \frac{b+\kappa}{m^2}\mathbf{\Delta}^{\mathrm{T}}$, $\tilde{\mathbf{C}}_u = \begin{pmatrix} \mathbf{E}\mathbf{D}_{\mathbf{c}}\mathbf{C} & \mathbf{E}\mathbf{C}_{\mathbf{c}} \end{pmatrix}$, $\tilde{\mathbf{C}}_y = \begin{pmatrix} \mathbf{C} & \mathbf{0}_2 \end{pmatrix}$, $\tilde{\mathbf{C}}_{uv} = \mathbf{E}\mathbf{D}_{\mathbf{c}}\mathbf{D}_v$ and $\tilde{\mathbf{C}}_{yv} = \mathbf{D}_v$ with $\mathbf{B}_z = \mathbf{B}_v\tilde{\mathbf{D}}_{oz} + \mathbf{B}_\gamma + \mathbf{A}\mathbf{B}_\delta$, $\tilde{\mathbf{D}}_{oz} = \frac{1}{m}\mathbf{\Delta}^{\mathrm{T}}$ and $\mathbf{E} = \begin{pmatrix} \mathbf{0}_{N,1} & \mathbf{I}_N \end{pmatrix}$. $\mathbf{0}_{i,j}$ (*resp.* $\mathbf{0}_k$) designates any $(i \times j)$-rectangular (*resp.* k-squared) null matrix and $\mathbf{I}_k$ is the identity matrix of order k , for all positive integers i, j, k.

For the proof, consider the state vector $\tilde{\mathbf{x}}^{\mathrm{T}} = \begin{pmatrix} \mathbf{x}^{\mathrm{T}} + \tilde{\mathbf{z}}^{\mathrm{T}}\mathbf{B}_\delta^{\mathrm{T}} \mid \mathbf{x}_{\mathbf{c}}^{\mathrm{T}} \end{pmatrix}$ of the closed-loop linear positioning sub-system (Σ_{LP}) and the new state variable $\bar{v} = \tilde{v} + \tilde{\mathbf{D}}_{oz}\tilde{\mathbf{z}}$ of the closed-loop linear observer sub-system (Σ_{LO}).

The closed-loop linear dynamics (Σ_{LP}) and (Σ_{LO}) are linked to the nonlinear friction estimation error dynamics (Σ_{NL}) by the feedback input vector $\mathbf{u}_z$ (see Fig. 2) throughout the property of passivity. As previously stated for the LuGre friction estimation [2], [3], partitioning the closed-loop system into linear and nonlinear parts and thanks to the passivity of the GMS model and the passivity theorem, we will derive conditions on the controller and the observer which guarantee the stability of the closed-loop system. The condition is that the resulting linear block (Σ_{L}) is SPR. Moreover, the main objective of the feedback servo-dynamics is to ensure a best trade-off between stability, accuracy and robustness of the positioning tracking subjected to the effect of different channels of disturbances (due to observation errors of unmeasurable states). So, additional criteria encompassing various performances of the closed-loop system (such as LMI-region stability constraints and H_∞ optimization) will be introduced to take into account robust stability and disturbance rejection aspects. All of these statements will be cast as feasibility and/or optimization LMI problems.

4. MULTI-OBJECTIVE CONTROLLER DESIGN - LMI APPROACH

Thanks to the passivity of the GMS friction model and by using the passivity theorem [9], we partition the closed-loop system into linear (reduced-observer and positioning tracking) and nonlinear (friction dynamics) subsystems and we will derive conditions on the controller (K) and the observer gain κ which guarantee the stability of the overall closed-loop system. In addition, the effect of the velocity estimate dynamics is cast inside the friction compensation dynamics and the position tracking as hierarchical systems.

In this section, we investigate the stability condition of the overall system dynamics subject to a specific closed-loop pole clustering and an H_∞ optimization design to limit the sensitivity of the tracking error output to the friction and velocity estimation errors. The stated problems will be tractably solved using the LMI formalism which can easily be solved by using any interior point optimization method implemented in the ©MATLAB software using the LMI control toolbox [7].

4.1 Stability condition

Consider the set of the interconnected systems (11), (12), (20) $\sim$ (22). In the following, we establish the stability condition by assuming $\omega_z = \mathbf{0}_{N,1}$ and $\omega_d = 0$ (noting that the response of an asymptotically stable system, which is disturbed by exogenous bounded signals, is a combination of an asymptotically reducing response and a bounded disturbance). Note that from now on, the symbol $\star$ replaces blocks in the matrix inequalities that are readily inferred by symmetry.

Proposition 2: For any positive definite and symmetric matrix $\mathbf{\Lambda}$, the nonlinear friction observer, reduced-order velocity observer and position tracking errors are asymptotically stable if there exist a matrix $\tilde{\mathbf{P}}_s = \tilde{\mathbf{P}}_s^{\mathrm{T}} > 0$ and a scalar $\pi_s > 0$, such that

$$\begin{pmatrix} \tilde{\mathbf{P}}_s\tilde{\mathbf{A}} + \tilde{\mathbf{A}}^{\mathrm{T}}\tilde{\mathbf{P}}_s & \star & \star \\ \tilde{\mathbf{B}}_v^{\mathrm{T}}\tilde{\mathbf{P}}_s & 2\pi_s\tilde{A}_o & \star \\ \tilde{\mathbf{B}}_z^{\mathrm{T}}\tilde{\mathbf{P}}_s - \mathbf{\Lambda}\tilde{\mathbf{C}}_u & \pi_s\tilde{\mathbf{B}}_{oz}^{\mathrm{T}} - \mathbf{\Lambda}\tilde{\mathbf{C}}_{uv} & \mathbf{0}_N \end{pmatrix} \leq 0 \quad (23)$$

For the proof, assume $\omega_z = \mathbf{0}_{N,1}$ and $\omega_d = 0$, consider the following Lyapunov function candidate:

$$V(t) = \tilde{\mathbf{x}}^{\mathrm{T}}\tilde{\mathbf{P}}_s\tilde{\mathbf{x}} + \pi_s\bar{v}^2 + \tilde{\mathbf{z}}^{\mathrm{T}}\mathbf{\Lambda}\tilde{\mathbf{z}} \quad (24)$$

and use Eqs. (11) $\sim$ (13). Then, the inequality (23) implies $\dot{V} \leq 0$. By using the Kalman-Yakubovich-Popov lemma [9], the transfer matrix loop between $(-\tilde{\mathbf{z}})$ and $\mathbf{u}_z$ given by Eqs. (20) and (21) is SPR, and:

$$\begin{pmatrix} \tilde{\mathbf{P}}_s\tilde{\mathbf{A}} + \tilde{\mathbf{A}}^{\mathrm{T}}\tilde{\mathbf{P}}_s & \star \\ \tilde{\mathbf{B}}_v^{\mathrm{T}}\tilde{\mathbf{P}}_s & 2\pi_s\tilde{A}_o \end{pmatrix} < 0 \quad (25)$$

$$\tilde{\mathbf{B}}_z^{\mathrm{T}}\tilde{\mathbf{P}}_s = \mathbf{\Lambda}\tilde{\mathbf{C}}_u \quad (26)$$

$$\pi_s\tilde{\mathbf{B}}_{oz}^{\mathrm{T}} = \mathbf{\Lambda}\tilde{\mathbf{C}}_{uv} \quad (27)$$

Now, let $S = \{\begin{pmatrix} \tilde{\mathbf{x}} \\ \bar{v} \\ -\tilde{\mathbf{z}} \end{pmatrix} | \dot{V} = 0\}$. Using Eqs. (25) $\sim$ (27), note that $\dot{V} = 0$ implies $\begin{pmatrix} \tilde{\mathbf{x}}(t) \\ \bar{v}(t) \end{pmatrix} \equiv \mathbf{0} \Rightarrow \begin{pmatrix} \dot{\tilde{\mathbf{x}}}(t) \\ \dot{\bar{v}}(t) \end{pmatrix} \equiv \mathbf{0} \Rightarrow \tilde{\mathbf{z}} \equiv \mathbf{0}$. Therefore, the only solution that can stay identically in S is the solution $\begin{pmatrix} \tilde{\mathbf{x}} \\ \bar{v} \\ -\tilde{\mathbf{z}} \end{pmatrix} \equiv \mathbf{0}$. Thus, using the corollary 4.2 of [9], the overall closed-loop dynamics, stated by Eqs. (11), (20) and (21), is asymptotically stable.

4.2 Multi-objective design

Furthermore, we can design a controller which ensures the SPR condition given by Eq. (23) while assigning the closed-loop linear dynamics poles in any LMI region of the complex left-half plane [7], [8]. These augmented constraints on the eigenvalue clustering can be used to enforce some response specifications like the stability margin, the settling time, the overshot and the frequency response limits of these linear sub-systems.

To upper-limit the stability margin of the reduced-observer feedback loop (Σ_{LO}), we establish that the reduced-order velocity observer error exponentially converges to zero with rate of ζ if, for any $\zeta > 0$, there exists a scalar $\pi_e > 0$ such that [8]

$$2\pi_e\tilde{A}_o + 2\pi_e\zeta < 0 \quad (28)$$

For prevent fast observer dynamics (*i.e.* frequency of oscillatory modes), we propose to bunch the closed-loop observer (Σ_{LO}) pole in the disk of radius r_o centered at the origin. The LMI characterization for this stability region is now expressed as $\exists\pi_r > 0$, such that [8]

$$\begin{pmatrix} -r_o\pi_r & \star \\ \pi_r\tilde{A}_o & -r_o\pi_r \end{pmatrix} < 0 \quad (29)$$

To minimize the H_∞ norms of the closed-loop transfers from $(-\tilde{\mathbf{z}})$ and ω_d to $\tilde{v}$ respectively, which are used to ensure a disturbance rejection performance on the reduced-observer velocity error dynamics (Σ_{LO}), the following characterizations are now expressed for scalars $\pi_{\infty_1} > 0$ and $\pi_{\infty_2} > 0$ [8]

$$\begin{pmatrix} 2\tilde{A}_o\pi_{\infty_1} & \star & \star \\ \pi_{\infty_1}\tilde{\mathbf{B}}_{oz}^{\mathrm{T}} & -\rho_1\mathbf{I}_N & \star \\ 1 & \tilde{\mathbf{D}}_{oz} & -\rho_1 \end{pmatrix} < 0 \tag{30}$$

and

$$\begin{pmatrix} 2\tilde{A}_o\pi_{\infty_2} & \star & \star \\ \pi_{\infty_2}\tilde{B}_{od} & -\rho_2 & \star \\ 1 & 0 & -\rho_2 \end{pmatrix} < 0 \tag{31}$$

For prevent fast controller dynamics (*i.e.* frequency of oscillatory modes), we propose to bunch the closed-loop poles of the positioning error dynamics (Σ_{LP}) in the disk of radius r centered at the origin. The LMI characterization for this stability region is now expressed as $\exists\tilde{\mathbf{P}}_r = \tilde{\mathbf{P}}_r^{\mathrm{T}} > 0$, such that [8]

$$\begin{pmatrix} -r\tilde{\mathbf{P}}_r & \star \\ \tilde{\mathbf{P}}_r\tilde{\mathbf{A}} & -r\tilde{\mathbf{P}}_r \end{pmatrix} < 0 \tag{32}$$

Finally, we intent to minimize the H_∞ norm of the closed-loop transfer from $\omega_\infty = \begin{pmatrix} (-\tilde{\mathbf{z}})^{\mathrm{T}} & \omega_d \end{pmatrix}^{\mathrm{T}}$ to $\mathbf{y}$, which is used to ensure a disturbance rejection performance. This characterization is now expressed as follows [7]: for $\tilde{\mathbf{P}}_\infty = \tilde{\mathbf{P}}_\infty^{\mathrm{T}} > 0$

$$\begin{pmatrix} \tilde{\mathbf{A}}^{\mathrm{T}}\tilde{\mathbf{P}}_\infty + \tilde{\mathbf{P}}_\infty\tilde{\mathbf{A}} & \star & \star \\ \tilde{\mathbf{B}}_\omega^{\mathrm{T}}\tilde{\mathbf{P}}_\infty & -\rho_3\mathbf{I}_{N+1} & \star \\ \tilde{\mathbf{C}}_y & \mathbf{0}_{2,N+1} & -\rho_3\mathbf{I}_2 \end{pmatrix} < 0 \tag{33}$$

with $\tilde{\mathbf{B}}_\omega = \begin{pmatrix} \tilde{\mathbf{B}}_z & \tilde{\mathbf{B}}_d \end{pmatrix}$.

With the matrix inequality formulations (23), (28) $\sim$ (33), the controller/observer design problem can be stated as follows:
For any α_1, α_2 and α_3, minimize $\sum_{j=1}^{3}\alpha_j\|\mathrm{H}\|_{\infty_j}$, such that $\pi_e > 0$, $\pi_r > 0$, $\pi_s > 0$, $\pi_{\infty_1} > 0$, $\pi_{\infty_2} > 0$, $\tilde{\mathbf{P}}_r = \tilde{\mathbf{P}}_r^{\mathrm{T}} > 0$, $\tilde{\mathbf{P}}_s = \tilde{\mathbf{P}}_s^{\mathrm{T}} > 0$, $\tilde{\mathbf{P}}_\infty = \tilde{\mathbf{P}}_\infty^{\mathrm{T}} > 0$, κ, $\mathbf{A_c}$, $\mathbf{B_c}$, $\mathbf{C_c}$ and $\mathbf{D_c}$ satisfy the inequalities (23), (28) $\sim$ (33).

This problem is not tractable using the LMI formulation unless we require that the same Lyapunov matrix $\tilde{\mathbf{P}}$ and scalar π satisfy the inequalities (23), (28) $\sim$ (33). We therefore restrict our attention to the following conservative formulation [7]:
For any α_1, α_2 and α_3, minimize $\sum_{j=1}^{3}\alpha_j\rho_j$, such that $\pi > 0$, $\tilde{\mathbf{P}} = \tilde{\mathbf{P}}^{\mathrm{T}} > 0$, κ, $\mathbf{A_c}$, $\mathbf{B_c}$, $\mathbf{C_c}$ and $\mathbf{D_c}$ satisfy the constarints (23), (28) $\sim$(33), with

$$\begin{array}{l} \tilde{\mathbf{P}} = \tilde{\mathbf{P}}_r = \tilde{\mathbf{P}}_s = \tilde{\mathbf{P}}_\infty \\ \pi = \pi_e = \pi_r = \pi_s = \pi_{\infty_1} = \pi_{\infty_2} \end{array} \tag{34}$$

4.3 Output feedback synthesis

The conditions for design of the controller/observer given in the previous section are bilinear in the variables π, κ, $\tilde{\mathbf{P}}$, $\mathbf{A_c}$, $\mathbf{B_c}$, $\mathbf{C_c}$ and $\mathbf{D_c}$. By using the linearizing change of controller variables introduced in [7], we convert these bilinear matrix inequalities (BMIs) into LMIs in a different set of variables.

Partition $\tilde{\mathbf{P}}$ and $\tilde{\mathbf{P}}^{-1}$ as:

$$\tilde{\mathbf{P}} = \begin{pmatrix} \mathbf{P} & \mathbf{M} \\ \mathbf{M}^{\mathrm{T}} & \mathbf{R} \end{pmatrix};\ \tilde{\mathbf{P}}^{-1} = \begin{pmatrix} \mathbf{Q} & \mathbf{N} \\ \mathbf{N}^{\mathrm{T}} & \mathbf{S} \end{pmatrix} \tag{35}$$

with $\mathbf{P} = \mathbf{P}^{\mathrm{T}}$, $\mathbf{Q} = \mathbf{Q}^{\mathrm{T}}$ and such that the invertible matrices $\mathbf{M}$ and $\mathbf{N}$ satisfy

$$\mathbf{M}\mathbf{N}^{\mathrm{T}} = \mathbf{I} - \mathbf{P}\mathbf{Q} \tag{36}$$

Let the new stated matrical variables $\hat{\mathbf{A}}$, $\hat{\mathbf{B}}$, $\hat{\mathbf{C}}$ and $\hat{\mathbf{D}}$ be given by:

$$\left\{ \begin{array}{ll} \hat{\mathbf{A}} = & \mathbf{M}\mathbf{A_c}\mathbf{N}^{\mathrm{T}} + \mathbf{M}\mathbf{B_c}\mathbf{C}\mathbf{Q} + \mathbf{P}\mathbf{B}\mathbf{C_c}\mathbf{N}^{\mathrm{T}} + \\ & \mathbf{P}\mathbf{A}\mathbf{Q} + \mathbf{P}\mathbf{B}\mathbf{D_c}\mathbf{C}\mathbf{Q} \\ \hat{\mathbf{B}} = & \mathbf{M}\mathbf{B_c} + \mathbf{P}\mathbf{B}\mathbf{D_c} \\ \hat{\mathbf{C}} = & \mathbf{C_c}\mathbf{N}^{\mathrm{T}} + \mathbf{D_c}\mathbf{C}\mathbf{Q} \\ \hat{\mathbf{D}} = & \mathbf{D_c} \end{array} \right. \tag{37}$$

Proposition 3: A full-order output-feedback controller ($\mathbf{K}$), an observer gain κ, a symmetric matrix $\tilde{\mathbf{P}} > 0$ partitioned as in Eq. (35) and a scalar $\pi > 0$ exist such that the inequalities (23), (28) $\sim$ (33) hold if and only if matrices $\mathbf{P}$, $\mathbf{Q}$, $\hat{\mathbf{A}}$, $\hat{\mathbf{B}}$, $\hat{\mathbf{C}}$, $\hat{\mathbf{D}}$, scalars $\pi > 0$ and $\iota = \pi\kappa$ exist, such that the LMIs (39) $\sim$ (46) are feasible, with respect to the following objective function

$$\min \sum_{j=1}^{3}\alpha_j\rho_j \tag{38}$$

subject to

$$\begin{pmatrix} \mathbf{Q} & \star \\ \mathbf{I} & \mathbf{P} \end{pmatrix} > 0 \tag{39}$$

$$\begin{pmatrix} \mathbf{a}_{11} & \star & \star & \star \\ \mathbf{a}_{21} & \mathbf{a}_{22} & \star & \star \\ \mathbf{a}_{31} & \mathbf{a}_{32} & -2\frac{b}{m}\pi - \frac{2}{m}\iota & \star \\ \mathbf{a}_{41} & \mathbf{a}_{42} & \mathbf{a}_{N,1} - \mathbf{\Lambda}\mathbf{E}\hat{\mathbf{D}}\mathbf{D}_v & -\epsilon\mathbf{I}_N \end{pmatrix} < 0 \tag{40}$$

$$2(-\frac{b}{m} + \zeta_o)\pi - \frac{2}{m}\iota < 0 \tag{41}$$

$$\begin{pmatrix} r_o\pi & \star \\ \frac{b}{m}\pi + \frac{2}{m}\iota & r_o\pi \end{pmatrix} > 0 \tag{42}$$

$$\begin{pmatrix} -2\frac{b}{m}\pi - \frac{2}{m}\iota & \star & \star \\ \mathbf{a}_{N,1} & \rho_1\mathbf{I}_N & \star \\ 1 & \frac{1}{m}\mathbf{\Delta}^{\mathrm{T}} & -\rho_1 \end{pmatrix} < 0 \tag{43}$$

$$\begin{pmatrix} -2\frac{b}{m}\pi - \frac{2}{m}\iota & \star & \star \\ -\frac{1}{m}\pi & \rho_2 & \star \\ 1 & 0 & -\rho_2 \end{pmatrix} < 0 \tag{44}$$

$$\begin{pmatrix} -r\mathbf{Q} & \star & \star & \star \\ -r\mathbf{I} & -r\mathbf{P} & \star & \star \\ \mathbf{A}\mathbf{Q} + \mathbf{B}\hat{\mathbf{C}} & \mathbf{A} + \mathbf{B}\hat{\mathbf{D}}\mathbf{C} & -r\mathbf{Q} & \star \\ \hat{\mathbf{A}} & \mathbf{P}\mathbf{A} + \hat{\mathbf{B}}\mathbf{C} & -r\mathbf{I} & -r\mathbf{P} \end{pmatrix} < 0 \tag{45}$$

and

$$\begin{pmatrix} \mathbf{a}_{11} & \star & \star & \star \\ \mathbf{a}_{21} & \mathbf{a}_{22} & \star & \star \\ \mathbf{B}_\omega^{\mathrm{T}} & \mathbf{B}_\omega^{\mathrm{T}}\mathbf{P} & -\rho_3\mathbf{I}_{N+1} & \star \\ \mathbf{C}\mathbf{Q} & \mathbf{C} & \mathbf{0}_2 & -\rho_3\mathbf{I}_2 \end{pmatrix} < 0 \tag{46}$$

where $\mathbf{a}_{11} = \mathbf{A}\mathbf{Q} + \mathbf{Q}\mathbf{A}^{\mathrm{T}} + \mathbf{B}\hat{\mathbf{C}} + (\mathbf{B}\hat{\mathbf{C}})^{\mathrm{T}}$, $\mathbf{a}_{21} = \hat{\mathbf{A}} + (\mathbf{A} + \mathbf{B}\hat{\mathbf{D}}\mathbf{C})^{\mathrm{T}}$, $\mathbf{a}_{22} = \mathbf{P}\mathbf{A} + \mathbf{A}^{\mathrm{T}}\mathbf{P} + \hat{\mathbf{B}}\mathbf{C} + (\hat{\mathbf{B}}\mathbf{C})^{\mathrm{T}}$, $\mathbf{a}_{31} = (\mathbf{B}_v + \mathbf{B}\hat{\mathbf{D}}\mathbf{D}_v)^{\mathrm{T}}$, $\mathbf{a}_{32} = \mathbf{B}_v^{\mathrm{T}}\mathbf{P} + \mathbf{D}_v^{\mathrm{T}}\hat{\mathbf{B}}^{\mathrm{T}}$, $\mathbf{a}_{41} = \mathbf{B}_z^{\mathrm{T}} - \mathbf{\Lambda}\mathbf{E}\hat{\mathbf{C}}$, $\mathbf{a}_{42} = \mathbf{B}_z^{\mathrm{T}}\mathbf{P} - \mathbf{\Lambda}\mathbf{E}\hat{\mathbf{D}}\mathbf{C}$ and $\mathbf{a}_{N,1} = (\frac{1}{m}\mathbf{\Gamma} - \frac{b}{m^2}\mathbf{\Delta})\pi - \frac{1}{m^2}\mathbf{\Delta}\iota$, with $\mathbf{B}_\omega = \begin{pmatrix} \mathbf{B}_z & \mathbf{B}_d \end{pmatrix}$. The positive real ϵ in the LMI (40) is chosen too small in order to approximate the semi-positiveness by using the LMI toolbox instead of any extra semi-positive definite (SPD) technique.

For the proof, see *e.g.* [7]. The matrices $\mathbf{A_c}$, $\mathbf{B_c}$, $\mathbf{C_c}$ and $\mathbf{D_c}$ can easily be derived from Eq. (37) by calculating invertible matrices $\mathbf{M}$ and $\mathbf{N}$ satisfying Eq. (36).

The LMI optimization (38)-(46) can easily be solved by using any interior point optimization method implemented in the ©MATLAB software using the LMI control toolbox.

5. NUMERICAL SIMULATIONS

Some simulations are performed to illustrate the effectiveness of the proposed controller using a mono-stage GMS model with $b = 0.4$ N, $C = 10^{-3}$m/s, $f_c = 1$ N, $f_s = 1.5$ N, $m = 1$ Kg, $\gamma = 10^5$ N/m, $\delta = \sqrt{10^5}$ Ns/m, $\delta_s = 2$ and $\theta_s^{-1} = 10^{-6}$ m/s. We calculate the observer gain κ and the LTI compensator (K) for $k_s = 5$, $r = 10$, $r_o = 20$, $\zeta_o = 10$, the approximating parameter $\epsilon = 10^{-11}$ and the scaling parameter matrix $\mathbf{\Lambda} = 10^{10}$. Smooth trajectories with sinusoidal and quadratic shapes are used to show the tracking performance (see Fig. 3 and 4). The tracking errors decrease and are ultimately bounded. The feedback model predicts the actual state evolution while spending reasonable control amplitudes.

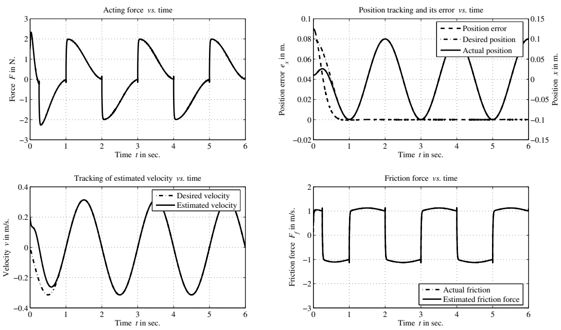

Fig. 3 Simulation results for sine trajectory.

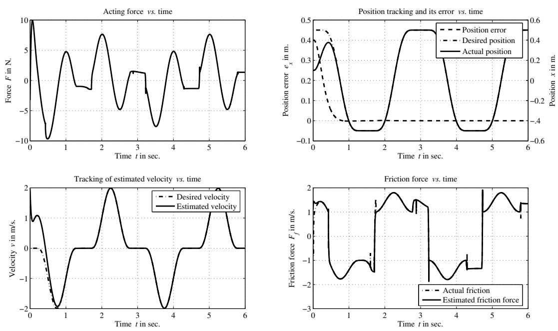

Fig. 4 Simulation results for quadratic trajectory.

6. CONCLUSION

In this paper, we develop a full-order dynamic output feedback positioning tracking for servo-systems with friction, based on GMS-friction observer dynamics. To this end, we use the position measurements and the estimated velocity magnitudes obtained by a reduced-order observer. An LTI compensator is appropriately calculated using the LMI approach to ensure multi-objective conditions on the designed interconnected dynamics. So, we are going on to show that the feasibility of the proposed method is ensured under 'several' multi-objective constraints, thanks to the high degree of flexibility of the LTI compensator and the performances of the LMI tools. Finally, the assumption that the friction model and its parameters are known exactly is to be regarded as a strong one. This provides us with the motivation in our future work to look at these realistic hypotheses without relying on costly adaptive schemes.

REFERENCES

[1] B. A.- Hélouvry, "A Survey of Models, Analysis Tools and Compensation Methods for the Control of Machines with Friction," *Automatica*, Vol. 30, No. 7, pp. 1083-1138, 1994.

[2] K. Khayati, P. Bigras and L.-A. Dessaint, "A Multi-stage Position/Force Control for Constrained Robotic Systems with Friction: Joint-space Decomposition, Linearization and Multi-objective Observer/Controller Synthesis using LMI Formalism," *IEEE Transactions on Industrial Electronics*, Vol. 53, No. 5, pp. 1698-1712, 2006.

[3] K. Khayati, P. Bigras and L.-A. Dessaint, "A Multi-objective Output-feedback Controller for System with Friction," *IFAC Symposium on Cost Oriented Automation*, Gatineau/Ottawa, Canada, pp. 103-108, 2004.

[4] N. Mallon, N. v. d. Woum, D. Putra and H. Nijmeijer, "Friction Compensation in a Controlled One-Link Robot Using a Reduced-Order Observer," *IEEE Transactions on Control Systems Technology*, Vol. 14, No. 2, pp. 374-383, 2006.

[5] K. Khayati and P. Bigras, "A New Model-based Dynamic Feedback Control for Systems with Friction," *in ISIC. IEEE International Conference on Systems, Man and Cybernetics*, Montreal, Canada, pp. 2710-2715, 2007.

[6] F. A.-Bender, V. Lampaert and J. Swevers, "The Generalized Maxwell-Slip Model: A Novel Model for Friction Simulation and Compensation," *IEEE Transactions on Automatic Control*, Vol. 50, No. 11, pp. 1883-1887, 2005.

[7] C. Scherer, P. Gahinet and M. Chilali, "Multi-objective Output-Feedback Control via LMI Optimization," *IEEE Transactions on Automatic Control*, Vol. 42, No. 7, pp. 896-911, 1997.

[8] M. Chilali and P. Gahinet, "H_∞ Design with Pole Placement Constraints: An LMI Approach," *IEEE Transactions on Automatic Control*, vol. 41, pp. 358-367, 1996.

[9] H. K. Khalil, *Noninear Systems*, Prentice-Hall, NY, 2002.